CHAPTER TWO

Computational Models of Neuromodulation

Christopher R. Butson, PhD[1]
Departments of Neurology & Neurosurgery, Milwaukee, Wisconsin, USA
[1]Corresponding author: e-mail address: cbutson@mcw.edu

Contents

Abstract

As neuromodulation therapy has grown, so has the recognition that computational models can provide important insights into the design, operation, and clinical application of neurostimulation systems. Models of deep brain stimulation and spinal cord stimulation have advanced over recent decades from simple, stereotyped models to sophisticated patient-specific models that can incorporate many important details of the stimulation system and the attributes of individual subjects. Models have been used to make detailed predictions of the bioelectric fields produced during stimulation. These predictions have been used as a starting point for further analyses such as stimulation safety, neural response, neurostimulation system design, or clinical outcomes. This chapter provides a review of recent advances and anticipated future directions in computational modeling of neuromodulation.
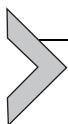
1. INTRODUCTION

Neuromodulation is commonly defined as the therapeutic alteration of activity in the nervous system by means of implanted devices. By this definition, cardiac pacemakers and cochlear implants are two of the most

successful neuromodulation therapies ever devised. The theory of operation behind cardiac pacemakers seems straightforward: the primary function of the heart is to pump blood through the circulatory system; cardiac tissue is electrically excitable, and electrical stimulation can be used to regulate the timing of heart contractions via an implantable system. Cochlear implants also have a clear theory of operation: the cochlea has a tonotopic organization of sensory neurons; neurons in the cochlea are electrically excitable, and electrical stimulation can be used to selectively stimulate cells in confined regions of the cochlea to mimic external sound energy in a particular frequency range. There are common themes in these two examples. First, we have a good understanding of the primary function of the target organ. Second, we have clear evidence of an excitatory response to electrical stimulation. Third, we have clear evidence that neuromodulation can be used to help reestablish or mimic the function of the healthy organ. Lastly, we have quantitative, objective measures of the efficacy of stimulation.

Over the past two decades there has been increasing interest in neuromodulation therapies such as: deep brain stimulation (DBS) for the treatment of Parkinson's disease (PD; Limousin et al., 1995), essential tremor (Benabid et al., 1996), and dystonia (Vidailhet et al., 2005) as well as potential new indications such as depression (Hamani & Nóbrega, 2010; Mayberg, 2009); and spinal cord stimulation (SCS) for treatment of many types of chronic pain (Cameron, 2004). However, in contrast to the examples mentioned above, the theory of operation behind DBS and SCS is not as well developed. First, in the context of the conditions that are treated using these therapies, we do not have a clear understanding of what the central nervous system (CNS), particularly the brain, is doing in its healthy state. Further, we often lack a detailed understanding of the pathophysiology of the disease state. Second, the effects of neuromodulation in the CNS have been shown to have a range of excitatory and inhibitory effects. Third, much of the evidence for the therapeutic effectiveness was gathered empirically without a clear mechanistic understanding. Lastly, in many cases we lack objective measures of the efficacy of stimulation and instead rely on subjective measures that are self-reported or assessed by an examiner.

Despite these apparent limitations there is evidence that large patient populations can be effectively treated using neuromodulation therapy, and this has fostered a sense of hope for new indications, some of which have few other treatment options. Computational models are being used with

increasing frequency in the study of neuromodulation and it is now clear that they can provide insights that would be difficult to obtain using other approaches. In particular, models are being used to fill many gaps in our knowledge about DBS and SCS. Where is stimulation occurring? How is it affecting nearby neural tissue? Why is a certain manner of stimulation effective or ineffective? Different types of models have been created to answer these questions, each with their own purpose. *Canonical models* are used to represent the functional properties of a system without necessarily attempting to mimic the details of the stimulation system or the neural tissue. These have been used to examine the pathophysiological features of the basal ganglia in diseases such as PD and to predict how neuromodulation systems could be interacting with the basal ganglia (Frank, Samanta, Moustafa, & Sherman, 2007; Rubin & Terman, 2004). *Bioelectric field models* are used to predict the bioelectric field produced in the body during neurostimulation based on a detailed geometric and biophysical characterization (Butson, Cooper, Henderson, & McIntyre, 2007). These models have been used to predict the spatial and temporal properties of stimulation. *Cellular models* are created to predict neural firing patterns in response to stimulation using detailed neuron geometries with Hodgkin–Huxley ion channel kinetics (Holsheimer, 1998). Computational models provide a way to characterize design decisions and treatment approaches before a system is manufactured and deployed. As always, final evidence of effectiveness comes from human clinical trials. However, it is infeasible to test the vast parameter space that exists in neuromodulation therapy using a trial-based approach in humans or animals–it is simply too large and clinical trials are far too expensive.

This chapter provides a review of the history, recent advances, and anticipated future directions in computational modeling of neuromodulation. Examples are presented in the areas of DBS for PD and SCS to treat chronic pain. They are organized around insights that have been gained from model-based approaches.
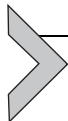
2. FOUNDATIONS OF NEUROSTIMULATION MODELING

Computational modeling of neuromodulation is an area that grew from computational neuroscience, which is a field of study that uses computational tools to understand how the nervous system solves problems, and from bioelectric field modeling, which is the study of the interactions of electromagnetic fields with biological tissue. The important distinction of

neuromodulation models is that they specifically account for perturbations to the nervous system that are caused by artificial stimulation using implanted electrodes. Current approaches to modeling have come about because of the confluence of advances in several areas. First, there have been substantial advances in quantitative characterization of the behavior of neural systems. An early example of this was the work of Hodgkin–Huxley (Hodgkin & Huxley, 1952), who won the Nobel Prize for their painstaking work in deriving a set of governing equations for the nonlinear behavior of selective ion channels in nerve membranes. Second, there has been a steady expansion in computational power available via commodity workstations, which has facilitated the use of computational tools. During this time finite element modeling (FEM) has matured as a numerical approach for solving bioelectric field problems with complex geometric features and anisotropic tissue properties. Also, open-source programs such as GENESIS (Beeman & Bower, 1998) and NEURON (Carnevale & Hines, 2006) have been written to simulate neurons using multicompartmental models with Hodgkin–Huxley ion channel kinetics. Third, we have developed a stronger conceptual understanding of the neural response to a variety of stimulation modalities and conditions. For example, textbooks are available that provide a broad theoretical basis for many types of neurostimulation therapy (Malmivuo & Plonsey, 1995). Lastly, seminal work by investigators such as Lorente de Nó, Rattay, Ranck and McNeal provided some of the foundations of modern computational models (Lorente de Nó, 1947; McNeal, 1976; Ranck, 1975; Rattay, 1986).

The common theory of operation behind DBS and SCS is that an applied electromagnetic field impinges on neural structures located in anatomical regions near the electrode(s), which in turn leads to a functional response. In the best case, a patient receives good therapeutic benefit with minimal side effects and this is a gratifying outcome for all involved. However, when neuromodulation therapy is ineffective we have had few tools at our disposal to determine why. Possibilities range from suboptimal lead location to inadequate titration of stimulation settings to misdiagnosis. Hence, computational models can provide a way to augment our understanding of neuromodulation therapy. To date, models have been developed to (1) predict the electric fields produced during stimulation; (2) predict the neural response to the applied electric field; (3) elucidate the dynamics of the CNS in the healthy and diseased state; (4) explore mechanisms of stimulation; and (5) quantify the interactions between the stimulation system and anatomical regions using patient-specific models generated from imaging

modalities such as magnetic resonance imaging (MRI), diffusion-weighted imaging (DWI), or computed tomography (CT).
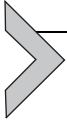
3. STIMULATION SAFETY

Computational modeling has been useful for assessing stimulation safety. Specifically, models have been used to estimate whether stimulation parameters fall within accepted guidelines for avoiding tissue damage. Much of this work is based on two fundamental pieces of information. First, early work by Lilly identified a class of charge-balanced waveforms that could be applied continuously to neural tissue without causing injury (Lilly, Hughes, Alvord, & Galkin,1955). These waveforms have two important properties: they consist of an initial cathodic or anodic pulse of fixed pulse width; and the initial pulse is quickly followed by a longer duration, lower amplitude pulse with an equal amount of charge (hence the name charge-balance waveform). Later, McCreery published data on safe stimulation limits based on data gathered from animal studies (McCreery, Agnew, Yuen, & Bullara, 1990). This data was later reinterpreted to provide an estimate of safe stimulation limits using parametric information based on charge quantity and charge density (Shannon, 1992). The idea behind this approach is that the safety of Lilly-type waveforms can be assessed by taking into account the average charge density over each electrode contact and the total charge per phase, both of which can be estimated with aid of computational models. Hence, models can provide an opportunity to assess the safety of novel stimulation systems or configurations of anodes and cathodes before they are used in practice. They have also been used to assess the degree to which current density is unevenly distributed across the surface of the electrode contact (Wei & Grill, 2005). Generally speaking, current preferentially flows through the edges of the electrodes rather than the center.
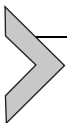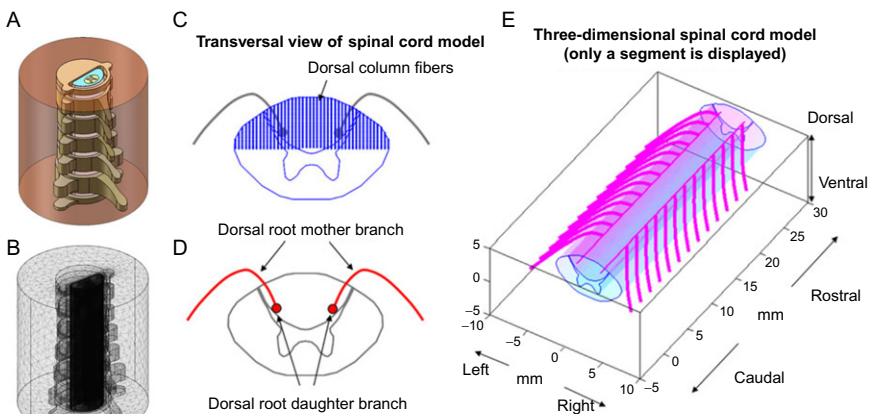
4. SPINAL CORD STIMULATION FOR PAIN

SCS has been used to treat pain associated with a variety of neuropathic and ischemic conditions (Cameron, 2004; Foletti, Durrer, & Buchser, 2007). Generally speaking, the mechanisms of action of SCS are not well understood and as a result its clinical application has been guided largely by observations regarding effective versus ineffective stimulation. For example, one common observation is that to achieve good pain relief, stimulation-induced paresthesias should overlap with the painful

region of the body. Another is that paresthesia "spreads" to multiple dermatomes as the pulse amplitude is increased (Hunter & Ashby, 1994) and that increasing pulse width to values as high as 500 or 1000 µs seems to be correlated with a caudal shift in coverage (Yearwood, Hershey, Bradley, & Lee, 2010). It is also believed that the therapeutic neural targets of SCS are axons in the dorsal column (DC), while activation of axons in the dorsal root (DR) is undesirable. Lastly, it is widely recognized that the thickness of the cerebrospinal fluid (CSF) layer in the spinal cord can vary over a wide range as a function of the spinal cord segment and the posture of the patient (Cameron & Alo, 1998), and this could have an effect on stimulation effectiveness. SCS models have been constructed to provide quantitative support for each of these observations.

The earliest example of an SCS model used a two-dimensional FEM to assess bipolar versus monopolar epidural stimulation (Coburn, 1980). FEM models have since been used in many studies to predict the electric field produced during neurostimulation using three-dimensional (3D) volumetric models (Fig. 2.1A) governed by the Poisson equation, which is equivalent to Ohm's Law in 3D space. The conceptual basis for these models is that stimulating electrodes serve as voltage or current sources that inject current through a resistive tissue medium. The Poisson equation can be solved either


Figure 2.1 Finite element models of spinal cord stimulation. (A) 3D FEM model of spinal cord segmented by tissue type. (B) Finite element mesh. (C) Cross-section of spinal cord model showing dorsal columns and (D) dorsal roots. (E) 3D FEM model of spinal cord. *Parts A and B modified from Hernández-Labrado et al. (2011). Parts C, D, and E modified from Lee et al. (2011).*

analytical or numerical. Analytical models are attractive because they usually provide a closed-form solution using a compact set of governing equations. However, such models exist for only a small collection of very simplified geometries. As a concrete example, analytical models exist for current or voltage sources in a conductive medium; the electrode is approximated by a point source and tissue is considered to be homogeneous and isotropic. This often provides a solution that is approximately correct at locations distant from the electrode. However, what is desired in neuromodulation models is often the exact opposite: we need a highly accurate solution in the region around the electrode but are often willing to accept reduced accuracy in locations distant from the source. Fortunately, numerical FEM models are designed to solve this class of problems. The distinguishing feature of FEM, and the basis for its name, is that the geometric features in the model are subdivided into tetrahedral (four sided) or hexahedral (six sided) elements that form a mesh. Meshes are often multiresolution, which means that the element size can change depending on the fineness of the geometry and the necessary solution accuracy. FEM models of SCS and DBS often use tetrahedral meshes with very small element sizes near the electrodes, where the voltage is changing the fastest, and much larger elements distant from the electrode where the voltage is changing more slowly. The major drawback of numerical FEM models is that they can require significant computational resources because one equation is required to represent each node in the mesh. Hence, the number of equations that must be simultaneously solved is directly proportional to the node density and mesh volume. Fortunately, it is possible to solve systems of up to a million equations using commodity workstations.

To assess the effects of SCS, early studies used FEM models to quantify simple outcome measures such as electric field magnitude, which is relatively easy to calculate but is not an accurate predictor of neural response. In the earliest model–based study, the authors examined the electric fields produced in the spine and concluded that field strength was much stronger for epidural than transdermal stimulation (Coburn, 1980). Later models incorporated more accurate predictors such as the activating function (Rattay, 1986), which is the second spatial derivate of the voltage along a neural element such as an axon. The activating function can also be calculated quickly and is a more accurate predictor of activation than the electric field alone. One early SCS study used the activating function to estimate neural response while assessing the effects of anisotropic tissue properties in model predictions (Struijk, Holsheimer, van Veen, & Boom, 1991). They

illustrated that the difference between the homogeneous and inhomogeneous model is mainly due to spreading of the current in longitudinal and lateral direction caused by the highly conductive CSF layer. However, the activating function suffers from important limitations such as the inability to easily incorporate time-dependent parameters including frequency or pulse width (Moffitt, McIntyre, & Grill, 2004). To address these limitations, several models combined FEM predictions of the electric field with multicompartmental models of individual neurons (McIntyre, Grill, Sherman, & Thakor, 2004). These are believed to provide the most accurate estimates of the response to stimulation as long as they are properly constrained with anatomical and physiological data. The integration of cellular models such as axons with the FEM allows a more detailed understanding of the interactions between the SCS system and nearby neural elements such as the DC and DR (Fig. 2.1B), but at the cost of much greater complexity.

SCS models have been used to disambiguate the effects of changing pulse width and amplitude. Since both of these parameters increase the amount of charge injected during each stimulation pulse, they might be expected to have similar effects. However, experimental and empirical observations have suggested that this is not the case. As a starting point there is a wealth of electrophysiological data that has been collected on strength–duration curves to establish the relationship between stimulation pulse duration and amplitude (Nowak & Bullier, 1998a, 1998b). The minimal amplitude necessary to excite a neural element is called rheobase; chronaxie is the pulse duration at twice rheobase. The chronaxie of myelinated axons is in the range 30–200 whereas dendrites and cell bodies are often much longer. These values have been measured electrophysiologically (Holsheimer, Demeulemeester, Nuttin, & de Sutter, 2000; Holsheimer, Dijkstra, Demeulemeester, & Nuttin, 2000) and have been estimated from patient studies (Rizzone et al., 2001) using stimulus–response data, providing an opportunity to make direct comparisons between *in vivo*, *in vitro*, and model data to characterize the neural targets of stimulation.
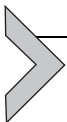
5. DEEP BRAIN STIMULATION FOR PARKINSON'S DISEASE

FEM models have been used to calculate the voltage distribution in the brain during DBS, and these models have illustrated several basic features. For example, conventional DBS electrode contacts implanted in the subthalamic nucleus (STN), internal segment of the globus pallidus (GPi), or thalamus have impedances of around $1000\,\Omega$ (Hemm et al.,

2004) which reflects the contributions of the wire, electrode–tissue interface and tissue itself. At typical stimulation settings for PD (monopolar, −3 V or −3 mA, 90 μs pulse width, 130 Hz), DBS creates a voltage distribution that ranges from −3 V at the electrode contact to near zero at the distant anode, which is the implantable pulse generator (IPG). Bipolar DBS with a single cathode and a single anode on the same lead creates a distribution that follows a gradient from about −1.5 V at the cathode to about +1.5 V at the anode, while the distant IPG is still near 0 V. These simple examples illustrate several basic concepts behind bioelectric field modeling. First, the body does not contain a "ground" electrode in the traditional sense nor does it contain reference or indifferent electrodes that are commonly used in electrophysiological recordings. Rather, DBS systems contain only anodes and cathodes. To account for this, FEM models use implicit or explicit mechanism to enforce a voltage of zero at locations distant from the electrode, which is meant to mimic the assumption that the average voltage within the body is zero at any time point. Second, the voltage gradient within the tissue can occur over short distances, such as between adjacent contacts during bipolar stimulation, or much longer distances such as between the electrode contact in the brain and the IPG in the torso during monopolar stimulation. Third, these models have been developed further to take into account the impedance of the encapsulation layer and the voltage drop that occurs at the electrode–tissue interface due to charge transfer from electrons in the metal electrode contact to ions in the tissue medium (Gimsa et al., 2005; Lempka, Miocinovic, Johnson, Vitek, & McIntyre, 2009). FEM models have suggested that the thickness and conductivity of the encapsulation layer is one of the primary determinants of electrode impedance and that there is a substantial voltage drop across the encapsulation tissue (Butson, Maks, & McIntyre, 2006).

However, as described these models only take into account the spatial voltage distribution in the tissue at the peak cathodic voltage, but do not take into account time. In fact, the Poisson equation does not explicitly contain a mechanism to incorporate the time-dependent properties such as the Lilly-type waveforms produced by the IPG. To address this, specialized solvers have been developed that allow prediction of the time- and space-dependent voltage distribution in the brain during DBS (Butson & McIntyre, 2005) and these predictions were later confirmed during *in vivo* recordings in primates (Miocinovic et al., 2009). These experiments and others have helped to illustrate several reasons why the signal that the brain "sees" is not an exact reproduction of the signal produced by the IPG. Decades of research in other fields such as electroencephalography have

guided us to think of the body as a purely resistive medium at frequencies below 1000 Hz, which is an assumption that has worked well for interpreting signals recorded from the skin. However, there are several reasons why this assumption might not be appropriate for neuromodulation models: neural tissue is known to have capacitive properties; stimulation electrodes are often made of a platinum–iridium alloy, which also has capacitive properties; and neurostimulation waveforms have substantial amounts of energy at frequencies above 1000 Hz. The existence of capacitance from the electrode or tissue, in combination with the resistive tissue properties, has the effect of creating a filter whose time constant is determined from the product of these values. This can transform the original waveform and reduce the amount of charge injected below what is expected from the IPG output alone.

FEM models are constructed using estimates of tissue properties derived from biological preparations (Gabriel, Gabriel, & Corthout, 1996; Geddes & Baker, 1967) which were then incorporated into parametric models of biophysical properties for a variety of different tissue types (Gabriel, Lau, & Gabriel, 1996). Later, DWI was used to measure water diffusivity in individual subjects. DWI data is often transformed into diffusion tensors (diffusion tensor imaging (DTI)), which provide a compact mathematical representation of the magnitude and anisotropy of diffusivity. DTI tensors are used to construct fiber tracts using tractography, and these have been incorporated into DBS models (Chaturvedi, Butson, Lempka, Cooper, & McIntyre, 2010). In addition, methods have been developed to estimate the conductivity of brain tissue from DTI (Tuch, Wedeen, Dale, George, & Belliveau, 2001). The major advantage of this approach is the ability to characterize anisotropic conductivity using diffusion tensors, which have been incorporated into patient-specific models (Butson et al., 2007).

Computation of the bioelectric field produced during DBS is a better-defined problem than predicting the neural response. The latter could be a function of many different attributes such as cell type and morphology, cell orientation within the induced bioelectric field, the complex biophysics of nonlinear ion channels in the cell membrane combined with the intracellular activity, and finally the synaptic connections that form neural circuits. And in contrast to SCS, the brain has a less stereotyped architecture than the spinal cord. One of the first insights to come from computational modeling was support for the idea that the neural targets of DBS are myelinated axons rather than cell bodies (Holsheimer, Demeulemeester, Nuttin, & de Sutter, 2000).

Hence, many of the combined FEM-cellular models of DBS examined the neural response of populations of myelinated axons as a measure of the extent to which DBS exerted it effects. A concept that emerged from these studies was the volume of tissue activated (VTA) in the brain during DBS in individual patients (Butson et al., 2007; McIntyre, Mori, Sherman, Thakor, & Vitek, 2004).

Patient-specific modeling is an approach that has grown substantially over the past decade (Fig. 2.2). As the name implies, these models are built to represent the anatomy and tissue properties of individual subjects. A common approach to this is to build a model from pre- and postoperative imaging. Preoperative MRI is used to identify the anatomy. This is co-registered with postoperative imaging such as MRI or CT to determine electrode location(s). In addition, DTI has been used to estimate tissue conductivity and to identify bundles of axonal fibers from tractography. Lastly, the models are often registered with a brain atlas to identify anatomical nuclei or other features that may not be visible using conventional imaging techniques. The product of this imaging is an anatomically accurate morphological model of the brain that can include the following features: the DBS lead; surface representation of nearby nuclei such as the STN, thalamus (with subthalamic nuclei such as the ventral intermediate (VIM)), or globus pallidus; fiber tracts identified from tractography or microscopic reconstruction techniques (Parent, Lévesque, & Parent, 2001); and voxel-based anisotropic tissue properties. These models can be used to quantify the electric field produced in the brain during DBS after taking into account the details of the stimulation protocol (stimulation waveform and configuration of anodes and cathodes). However, the electric field alone is not a good predictor of neural response to DBS. To address this, different approaches have been attempted including the activation function and the response of neural elements such as cell bodies or fibers of passage.

One idea that came from these models was the idea of a VTA produced during DBS. The idea behind this approach is that a criterion can be applied to determine which neurons reached threshold during DBS; neurons that reach threshold are considered part of the VTA. These volumes can be superimposed on patient-specific models to determine the overlap with nearby anatomical structures. A second idea was that VTAs could be combined with clinical outcomes from a cohort of patients to predict stimulation targets (Butson et al., 2011; Maks, Butson, Walter, Vitek, & McIntyre, 2009) which could be used to guide the selection of stimulation parameters

Patient-specific model
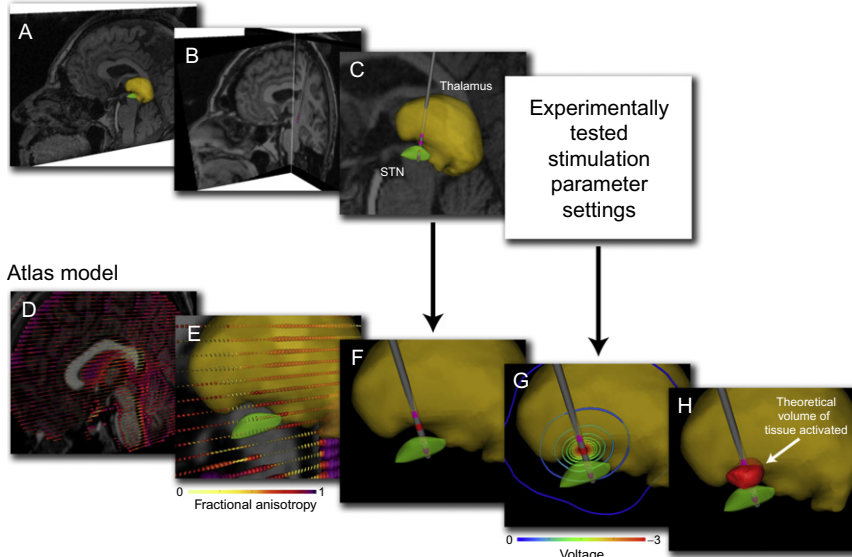
Atlas model

Probabilistic stimulation atlas
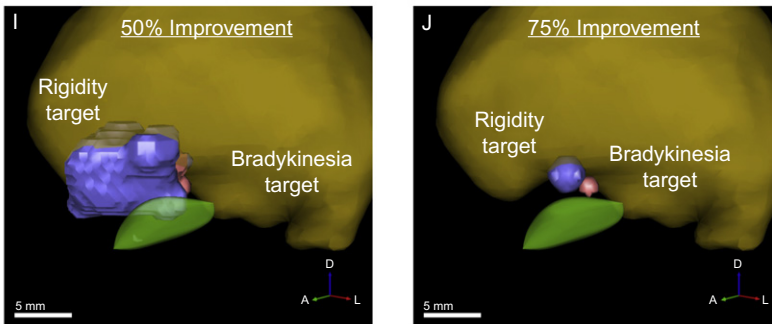
Figure 2.2 Patient-specific DBS models. (A) 3D nuclei (e.g., thalamus—yellow volume; STN—green volume) were fit to the preoperative MRI of each subject. (B) The preoperative MRI was coregistered with a postoperative MRI to identify the implanted DBS electrode location (note electrode in coronal slice). (C) For each hemisphere, the electrode location was defined relative to the pertinent nuclei. (D) Each patient-specific model was transformed into the context of a single atlas brain. The atlas brain included both anatomical and diffusion tensor imaging (DTI) data and was used to predict neural activation from the stimulation protocol. (E) DTI-based conductivity tensors with color indicating fractional anisotropy described the tissue electrical properties. (F) Each patient-specific model had a unique DBS electrode location. (G) Each experimentally tested stimulation parameter setting resulted in a unique voltage distribution. (H) The theoretical volume of tissue activated (VTA) for each DBS setting was calculated. (I and J) Probabilistic atlas of stimulation targets for bradykinesia (pink) and rigidity (blue) derived from a prospective evaluation of 163 VTAs from seven PD patients. *Modified from Butson, Cooper, Henderson, Wolgamuth, and McIntyre (2011).*

(Frankemolle et al., 2010). This has led to hope that computational models could be incorporated into clinical decision support systems (Butson et al., 2012).

Many of the DBS models described have used stimulation waveforms available in commercial IPGs. The design and selection of waveforms to best achieve therapeutic objectives remains a largely unexplored space. In this regard, models can aid in understanding how the waveforms produced by the stimulator interact with the pathophysiology of nearby nuclei in the basal ganglia. Recent work has suggested that the therapeutic effects of DBS are achieved using pulse trains at regular intervals, while irregularly space pulses had reduced effectiveness (Dorval, Kuncel, Birdno, Turner, & Grill, 2010). Lastly, computational basal ganglia models suggest that novel DBS waveforms exist which may return Parkinsonian network dynamics close to the normal state and exploit mechanisms that differ from those of conventional DBS at frequencies over 100 Hz (Feng, Greenwald, Rabitz, Shea-Brown, & Kosut, 2007).
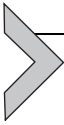
6. LIMITATIONS OF COMPUTATIONAL MODELS

Computational models have several inherent limitations. First, models can precisely quantify many different measures of neuromodulation, but in doing so there is a risk of overestimating the accuracy of predictions. The accuracy of model predictions depends on the degree to which it mimics the physiological system. Second, in contrast to physiological studies, computer simulations produce the same answer every single time unless sources of randomness are explicitly incorporated. As a result, it is often difficult for model-based analyses to characterize the uncertainty of *in vivo* systems. Hence, model-based results should be viewed cautiously until they can be constrained or validated with physiological data. Validation is a general approach by which model results are directly or indirectly compared to physiological data to establish accuracy, and as time goes one there is a growing expectation that model-based studies should include a validation mechanism. Fortunately, models of neuromodulation have become an accepted tool, a fact that has led many teams to conduct model experiments in conjunction with physiological studies.

7. CONCLUSIONS

Neuromodulation systems are growing in complexity. Systems are now becoming available with different electrical source types (voltage controlled and current controlled), increasing numbers and sizes of electrode

contacts, multiple independent sources and a growing range of stimulation waveforms. There is a perception that by virtue of these new capabilities, clinicians will have greater ability to customize therapy to each individual patient and as a result patient outcomes will improve. It is conceivable that this will occur and this is certainly what the medical, scientific, and commercial communities are hoping for. However, this is not a forgone conclusion. To achieve this goal we will need to expand our knowledge in at least three areas. First, we will need additional predictive power of the effects of stimulation as a function of location and type. Second, we will need additional information on the neurological targets of stimulation and the mechanisms of therapeutic improvement. Third, we will need decision support systems that provide a layer of abstraction between the clinician and patient such that stimulation protocols can be selected to provide a good match between the neurological objectives and the capabilities of the neuromodulation system. Computational models have the potential to fill gaps in our knowledge in each of these areas. Of these, the largest growth will likely be in the area of computational informatics systems that combine predictive models and interactive visualization for clinical decision making. Such systems have the potential to provide better patient outcomes and to accomplish this faster than would be achievable otherwise. To live up to this potential, future models will need to integrate simulation data with instrument-based measures, functional imaging, and clinical outcomes. From this view, models have an opportunity to synthesize new types of data and provide new insights that would be difficult to achieve otherwise.

ACKNOWLEDGMENTS & DISCLOSURES

REFERENCES

Beeman, D., & Bower, J. (1998). *The book of GENESIS: Exploring realistic neural models with the GEneral NEural SImulation System* (2nd ed.). New York, NY: Springer-Verlag.

Benabid, A. L., Pollak, P., Gao, D., Hoffmann, D., Limousin, P., Gay, E., et al. (1996). Chronic electrical stimulation of the ventralis intermedius nucleus of the thalamus as a treatment of movement disorders. *Journal of Neurosurgery, 84*(2), 203–214. http://dx.doi.org/10.3171/jns.1996.84.2.0203.

Butson, C. R., Cooper, S. E., Henderson, J. M., & McIntyre, C. C. (2007). Patient-specific analysis of the volume of tissue activated during deep brain stimulation. *NeuroImage, 34*(2), 661–670. http://dx.doi.org/10.1016/j.neuroimage.2006.09.034.

Butson, C. R., Cooper, S. E., Henderson, J. M., Wolgamuth, B., & McIntyre, C. C. (2011). Probabilistic analysis of activation volumes generated during deep brain stimulation. *NeuroImage*, *54*, 2096–2104. http://dx.doi.org/10.1016/j.neuroimage.2010.10.059.

Butson, C. R., Maks, C. B., & McIntyre, C. C. (2006). Sources and effects of electrode impedance during deep brain stimulation. *Clinical Neurophysiology: Official Journal of the International Federation of Clinical Neurophysiology*, *117*(2), 447–454. http://dx.doi.org/10.1016/j.clinph.2005.10.007.

Butson, C. R., & McIntyre, C. C. (2005). Tissue and electrode capacitance reduce neural activation volumes during deep brain stimulation. *Clinical Neurophysiology: Official Journal of the International Federation of Clinical Neurophysiology*, *116*(10), 2490–2500. http://dx.doi.org/10.1016/j.clinph.2005.06.023.

Butson, C. R., Tamm, G., Jain, S., Fogal, T., & Krüger, J. (2012). Evaluation of interactive visualization on mobile computing platforms for selection of deep brain stimulation parameters. *IEEE Transactions on Visualization and Computer Graphics* (In Press). http://doi.ieeecomputersociety.org/10.1109/TVCG.2012.92.

Cameron, T. (2004). Safety and efficacy of spinal cord stimulation for the treatment of chronic pain: A 20-year literature review. *Journal of Neurosurgery*, *100*(3 Suppl.), 254–267 Spine.

Cameron, T., & Alo, K. M. (1998). Effects of posture on stimulation parameters in spinal cord stimulation. *Neuromodulation: Journal of the International Neuromodulation Society*, *1*(4), 177–183. http://dx.doi.org/10.1111/j.1525-1403.1998.tb00014.x.

Carnevale, N. T., & Hines, M. L. (2006). *The NEURON book*. Cambridge: Cambridge University Press. http://dx.doi.org/10.1017/CBO9780511541612 Neuron (pp. 1–742).

Chaturvedi, A., Butson, C. R., Lempka, S. F., Cooper, S. E., & McIntyre, C. C. (2010). Patient-specific models of deep brain stimulation: Influence of field model complexity on neural activation predictions. *Brain Stimulation*, *3*(2), 65–67. http://dx.doi.org/10.1016/j.brs.2010.01.003.

Coburn, B. (1980). Electrical stimulation of the spinal cord: Two-dimensional finite element analysis with particular reference to epidural electrodes. *Medical and Biological Engineering and Computing*, *18*(5), 573–584.

Dorval, A. D., Kuncel, A. M., Birdno, M. J., Turner, D. A., & Grill, W. M. (2010). Deep brain stimulation alleviates parkinsonian bradykinesia by regularizing pallidal activity. *Journal of Neurophysiology*, *104*(2), 911–921. http://dx.doi.org/10.1152/jn.00103.2010.

Feng, X.-J., Greenwald, B., Rabitz, H., Shea-Brown, E., & Kosut, R. (2007). Toward closed-loop optimization of deep brain stimulation for Parkinson's disease: Concepts and lessons from a computational model. *Journal of Neural Engineering*, *4*(2), L14–L21. http://dx.doi.org/10.1088/1741-2560/4/2/L03.

Foletti, A., Durrer, A., & Buchser, E. (2007). Neurostimulation technology for the treatment of chronic pain: A focus on spinal cord stimulation. *Expert Review of Medical Devices*, *4*(2), 201–214. http://dx.doi.org/10.1586/17434440.4.2.201.

Frank, M. J., Samanta, J., Moustafa, A. A., & Sherman, S. J. (2007). Hold your horses: Impulsivity, deep brain stimulation, and medication in parkinsonism. *Science (New York, N.Y.)*, *318*(5854), 1309–1312. http://dx.doi.org/10.1126/science.1146157.

Frankemolle, A. M. M., Wu, J., Noecker, A. M., Voelcker-Rehage, C., Ho, J. C., Vitek, J. L., et al. (2010). Reversing cognitive–motor impairments in Parkinson's disease patients using a computational modelling approach to deep brain stimulation programming. *Brain: A Journal of Neurology*, *133*(Pt 3), 746–761. http://dx.doi.org/10.1093/brain/awp315.

Gabriel, C., Gabriel, S., & Corthout, E. (1996). The dielectric properties of biological tissues: I. Literature survey. *Physics in Medicine and Biology*, *41*(11), 2231–2249.

Gabriel, S., Lau, R., & Gabriel, C. (1996). The dielectric properties of biological tissues: II. Measurements in the frequency range 10 Hz to 20 GHz. *Physics in Medicine and Biology*, *41*, 2251.

Geddes, L. A., & Baker, L. E. (1967). The specific resistance of biological material—A compendium of data for the biomedical engineer and physiologist. *Medical and Biological Engineering*, *5*(3), 271–293.

Gimsa, J., Habel, B., Schreiber, U., van Rienen, U., Strauss, U., & Gimsa, U. (2005). Choosing electrodes for deep brain stimulation experiments—Electrochemical considerations. *Journal of Neuroscience Methods*, *142*(2), 251–265. http://dx.doi.org/10.1016/j.jneumeth.2004.09.001.

Hamani, C., & Nóbrega, J. N. (2010). Deep brain stimulation in clinical trials and animal models of depression. *The European Journal of Neuroscience*, *32*(7), 1109–1117. http://dx.doi.org/10.1111/j.1460-9568.2010.07414.x.

Hernández-Labrado, G. R., Polo, J. L., López-Dolado, E., & Collazos-Castro, J. E. (2011). Spinal cord direct current stimulation: finite element analysis of the electric field and current density. *Medical & Biological Engineering & Computing*, *49*, 417–429. http://dx.doi.org/10.1007/s11517-011-0756-9.

Hemm, S., Vayssiere, N., Mennessier, G., Cif, L., Zanca, M., Ravel, P., et al. (2004). Evolution of brain impedance in dystonic patients treated by GPI electrical stimulation. *Neuromodulation: Journal of the International Neuromodulation Society*, 7(2), 67–75. http://dx.doi.org/10.1111/j.1094-7159.2004.04009.x.

Hodgkin, A. L., & Huxley, A. F. (1952). A quantitative description of membrane current and its application to conduction and excitation in nerve. *The Journal of Physiology*, *117*(4), 500–544.

Holsheimer, J. (1998). Computer modelling of spinal cord stimulation and its contribution to therapeutic efficacy. *Spinal Cord*, *36*(8), 531–540.

Holsheimer, J., Demeulemeester, H., Nuttin, B., & de Sutter, P. (2000). Identification of the target neuronal elements in electrical deep brain stimulation. *The European Journal of Neuroscience*, *12*(12), 4573–4577.

Holsheimer, J., Dijkstra, E. A., Demeulemeester, H., & Nuttin, B. (2000). Chronaxie calculated from current-duration and voltage-duration data. *Journal of Neuroscience Methods*, *97*(1), 45–50.

Hunter, J. P., & Ashby, P. (1994). Segmental effects of epidural spinal cord stimulation in humans. *The Journal of Physiology*, *474*(3), 407–419.

Lee, D., Hershey, B., Bradley, K., & Yearwood, T. (2011). Predicted effects of pulse width programming in spinal cord stimulation: a mathematical modeling study. *Medical & Biological Engineering & Computing*, *49*, 765–774. http://dx.doi.org/10.1007/s11517-011-0780-9.

Lempka, S. F., Miocinovic, S., Johnson, M. D., Vitek, J. L., & McIntyre, C. C. (2009). In vivo impedance spectroscopy of deep brain stimulation electrodes. *Journal of Neural Engineering*, *6*(4), 046001. http://dx.doi.org/10.1088/1741-2560/6/4/046001.

Lilly, J. C., Hughes, J. R., Alvord, E. C., & Galkin, T. W. (1955). Brief, noninjurious electric waveform for stimulation of the brain. *Science (New York, N.Y.)*, *121*(3144), 468–469.

Limousin, P., Pollak, P., Benazzouz, A., Hoffmann, D., Le Bas, J. F., Broussolle, E., et al. (1995). Effect of parkinsonian signs and symptoms of bilateral subthalamic nucleus stimulation. *The Lancet*, *345*(8942), 91–95.

Lorente de Nó, R. (1947). *A study of nerve physiology*. Rockefeller Institute for Medical Research.

Maks, C. B., Butson, C. R., Walter, B. L., Vitek, J. L., & McIntyre, C. C. (2009). Deep brain stimulation activation volumes and their association with neurophysiological mapping and therapeutic outcomes. *Journal of Neurology, Neurosurgery, and Psychiatry*, *80*(6), 659–666. http://dx.doi.org/10.1136/jnnp. 2007.126219.

Malmivuo, J. A., & Plonsey, R. (1995). *Bioelectromagnetism: Principles and applications of bioelectric and biomagnetic fields*. New York, NY: Oxford University Press.

Mayberg, H. S. (2009). Targeted electrode-based modulation of neural circuits for depression. *The Journal of Clinical Investigation*, *119*(4), 717–725. http://dx.doi.org/10.1172/JCI38454.

McCreery, D. B., Agnew, W. F., Yuen, T. G., & Bullara, L. (1990). Charge density and charge per phase as cofactors in neural injury induced by electrical stimulation. *IEEE Transactions on Biomedical Engineering*, *37*(10), 996–1001.

McIntyre, C. C., Grill, W. M., Sherman, D. L., & Thakor, N. V. (2004). Cellular effects of deep brain stimulation: Model-based analysis of activation and inhibition. *Journal of Neurophysiology*, *91*(4), 1457–1469. http://dx.doi.org/10.1152/jn.00989.2003.

McIntyre, C. C., Mori, S., Sherman, D. L., Thakor, N. V., & Vitek, J. L. (2004). Electric field and stimulating influence generated by deep brain stimulation of the subthalamic nucleus. *Clinical Neurophysiology: Official Journal of the International Federation of Clinical Neurophysiology*, *115*(3), 589–595. http://dx.doi.org/10.1016/j.clinph.2003.10.033.

McNeal, D. R. (1976). Analysis of a model for excitation of myelinated nerve. *IEEE Transactions on Biomedical Engineering*, *23*(4), 329–337.

Miocinovic, S., Lempka, S. F., Russo, G. S., Maks, C. B., Butson, C. R., Sakaie, K. E., et al. (2009). Experimental and theoretical characterization of the voltage distribution generated by deep brain stimulation. *Experimental Neurology*, *216*(1), 166–176. http://dx.doi.org/10.1016/j.expneurol.2008.11.024.

Moffitt, M. A., McIntyre, C. C., & Grill, W. M. (2004). Prediction of myelinated nerve fiber stimulation thresholds: Limitations of linear models. *IEEE Transactions on Biomedical Engineering*, *51*(2), 229–236. http://dx.doi.org/10.1109/TBME.2003.820382.

Nowak, L. G., & Bullier, J. (1998a). Axons, but not cell bodies, are activated by electrical stimulation in cortical gray matter. II. Evidence from selective inactivation of cell bodies and axon initial segments. *Experimental Brain Research*, *118*(4), 489–500. http://dx.doi.org/10.1007/s002210050304.

Nowak, L. G., & Bullier, J. (1998b). Axons, but not cell bodies, are activated by electrical stimulation in cortical gray matter. I. Evidence from chronaxie measurements. *Experimental Brain Research*, *118*(4), 477–488. http://dx.doi.org/10.1007/s002210050304.

Parent, M., Lévesque, M., & Parent, A. (2001). Two types of projection neurons in the internal pallidum of primates: Single-axon tracing and three-dimensional reconstruction. *The Journal of Comparative Neurology*, *439*(2), 162–175.

Ranck, J. B. (1975). Which elements are excited in electrical stimulation of mammalian central nervous system: A review. *Brain Research*, *98*(3), 417–440.

Rattay, F. (1986). Analysis of models for external stimulation of axons. *IEEE Transactions on Biomedical Engineering*, *33*(10), 974–977. http://dx.doi.org/10.1109/TBME.1986.325670.

Rizzone, M., Lanotte, M., Bergamasco, B., Tavella, A., Torre, E., Faccani, G., et al. (2001). Deep brain stimulation of the subthalamic nucleus in Parkinson's disease: Effects of variation in stimulation parameters. *Journal of Neurology, Neurosurgery, and Psychiatry*, *71*(2), 215–219.

Rubin, J. E., & Terman, D. (2004). High frequency stimulation of the subthalamic nucleus eliminates pathological thalamic rhythmicity in a computational model. *Journal of Computational Neuroscience*, *16*(3), 211–235. http://dx.doi.org/10.1023/B:JCNS.0000025686.47117.67.

Shannon, R. V. (1992). A model of safe levels for electrical stimulation. *IEEE Transactions on Biomedical Engineering*, *39*(4), 424–426.

Struijk, J. J., Holsheimer, J., van Veen, B. K., & Boom, H. B. (1991). Epidural spinal cord stimulation: Calculation of field potentials with special reference to dorsal column nerve fibers. *IEEE Transactions on Biomedical Engineering*, *38*(1), 104–110. http://dx.doi.org/10.1109/10.68217.

Tuch, D. S., Wedeen, V. J., Dale, A. M., George, J. S., & Belliveau, J. W. (2001). Conductivity tensor mapping of the human brain using diffusion tensor MRI. *Proceedings of the*

National Academy of Sciences of the United States of America, *98*(20), 11697–11701. http://dx.doi.org/10.1073/pnas.171473898.

Vidailhet, M., Vercueil, L., Houeto, J.-L., Krystkowiak, P., Benabid, A.-L., Cornu, P., et al. (2005). Bilateral deep-brain stimulation of the globus pallidus in primary generalized dystonia. *The New England Journal of Medicine*, *352*(5), 459–467. http://dx.doi.org/10.1056/NEJMoa042187.

Wei, X. F., & Grill, W. M. (2005). Current density distributions, field distributions and impedance analysis of segmented deep brain stimulation electrodes. *Journal of Neural Engineering*, *2*(4), 139–147. http://dx.doi.org/10.1088/1741-2560/2/4/010.

Yearwood, T. L., Hershey, B., Bradley, K., & Lee, D. (2010). Pulse width programming in spinal cord stimulation: A clinical study. *Pain Physician*, *13*(4), 321–335.